Chemistry & Biology, Vol. 12, 981–991, September, 2005, ©2005 Elsevier Ltd All rights reserved. DOI 10.1016/j.chembiol.2005.07.007

A Chemical Inhibitor Reveals the Role of Raf Kinase Inhibitor Protein in Cell Migration

Shoutian Zhu,[1] Kevin T. Mc Henry,[1] William S. Lane,[2] and Gabriel Fenteany[1,*]
[1]Department of Chemistry
University of Illinois, Chicago
Chicago, Illinois 60607
[2]Harvard Microchemistry and Proteomics Analysis Facility
Harvard University
Cambridge, Massachusetts 02138

Summary

Raf kinase inhibitor protein (RKIP) is a modulator of cell signaling that functions as an endogenous inhibitor of multiple kinases. We demonstrate here a positive role for RKIP in the regulation of cell locomotion. We discovered that RKIP is the relevant cellular target of locostatin, a cell migration inhibitor. Locostatin abrogates RKIP's ability to bind and inhibit Raf-1 kinase, and it acts by disrupting a protein-protein interaction, an uncommon mode of action for a small molecule. Small interfering RNA-mediated silencing of RKIP expression also reduces cell migration rate. Overexpression of RKIP converts epithelial cells to a highly migratory fibroblast-like phenotype, with dramatic reduction in the sensitivity of cells to locostatin. RKIP is therefore the compound's valid target and a key regulator of cell motility.

Introduction

We previously described the biological activity of the oxazolidinone derivative UIC-1005 [1]. We now rename this compound locostatin, after its ability to inhibit cell locomotion in multiple systems, and have identified its cellular protein targets, which we present here. Our interest in locostatin's mode of action arose from discovery of its inhibitory activity in a high-throughput assay for compounds that affect cell migration during wound closure in Madin-Darby canine kidney (MDCK) epithelial cell monolayers. This screen was performed as part of our effort to apply a chemical approach to understanding the pathways and machinery of cell motility, processes for which small-molecule inhibitors are presently limited, with the goal of discovering new chemical probes and possibly new proteins involved in cell migration (for a review, see [2]). Moreover, small molecules that modulate cell migration could be of therapeutic value: for instance, antimigratory compounds could be exploited as anticancer agents, since both tumor angiogenesis and metastasis depend on cell migration, while promigratory compounds could be used to improve wound healing or may have applications in tissue engineering. In this report, we show that the biologically relevant target of locostatin is Raf kinase inhibitor protein (RKIP), a nonenzymatic regulatory protein whose ability to interact with Raf kinase is disrupted by locostatin.

RKIP is a widely expressed modulator of the Raf kinase cascade and other signaling pathways (for reviews, see [3–5]). RKIP associates with and inhibits the kinase activity of Raf-1 kinase [6, 7]. Phosphorylation of RKIP by protein kinase C (PKC) switches RKIP from Raf-1 to G protein receptor coupled kinase 2 (GRK2) [8, 9]. RKIP has recently been found to interact with and antagonize the kinase activity of B-Raf as well [10], although Raf-1 activation in vivo may be more under the control of RKIP than B-Raf activation [11]. In addition, RKIP can inhibit activation of the transcriptional regulator nuclear factor κB (NFκB) by interacting with and inhibiting the activities of kinases involved in NFκB activation [12]. RKIP was originally isolated on the basis of its ability to bind phosphatidylethanolamine [13]. It is therefore also known as phosphatidylethanolamine binding protein (PEBP), and it can interact with other ligands as well, although the functional significance of these interactions is unclear (for reviews, see [3–5]). RKIP is also the precursor of hippocampal cholinergic neurostimulating peptide (for a review, see [14]).

Roles for RKIP in diverse biological processes, including nervous and cardiac functions, membrane biogenesis, and spermatogenesis, have been suggested (for reviews, see [3–5]). Furthermore, RKIP may play a negative role in prostate cancer metastasis [15]. In contrast, using a chemical approach to the discovery of biological function, we have discovered that RKIP is also involved in the positive regulation of epithelial cell migration.

Results and Discussion

Identification of Locostatin Binding Proteins

Locostatin (compound **1** in Figure 1A) strongly inhibits membrane protrusion and cell sheet migration, without affecting gross actin cytoskeletal structure in cells or salt-induced polymerization of pyrene-actin in vitro ([1] and data not shown). The compound also inhibits scatter of MDCK cells, induced by hepatocyte growth factor/scatter factor (HGF/SF), and migration of B16-BL6 murine melanoma cells, a highly invasive and metastatic cancer cell line, with comparable IC_{50} values (Table S1; see the Supplemental Data available with this article online). In contrast, locostatin has comparatively little subtoxic antimigratory effect on the less aggressive A549 human lung adenocarcinoma and MCF7 human breast adenocarcinoma cells (Table S1).

Since structure-activity relationships strongly suggested that the mechanism of action of locostatin involves covalent modification of a target molecule(s) (Table 1 and [1]), we decided to prepare a radioactively labeled version of the compound, [^{3}H]locostatin (**1*** in Figure 1B), to enable the detection and purification of the locostatin binding proteins. We found that [^{3}H]locostatin specifically and covalently modifies only four proteins in cytosolic MDCK cell extracts, with no de-

*Correspondence: fenteany@uic.edu

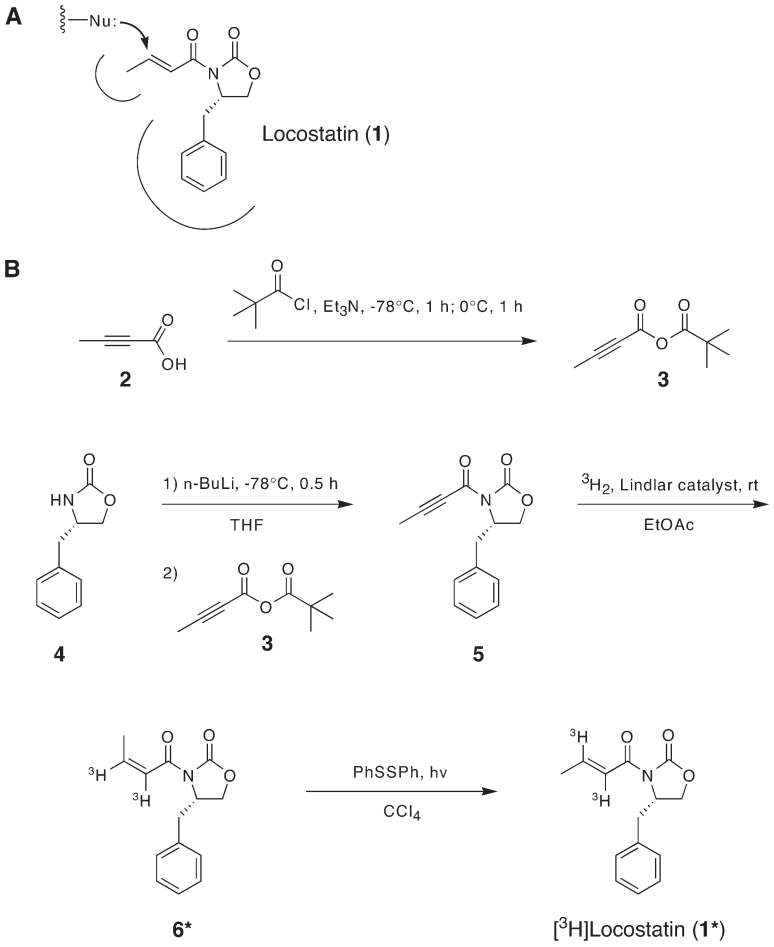

Figure 1. Putative Mode of Action of Locostatin and Synthesis of [^{3}H]Locostatin

(A) A nucleophilic residue (Nu:) on the target protein reacts with the electrophilic carbon of the Michael acceptor function of **1**, as indicated by the arrowhead, forming a covalent complex whereby the protein's activity is inhibited. Putative hydrophobic binding pockets are also shown. This model is supported by the structure-activity relationship data in Table 1 and the results showing that the interaction of compound with protein survives denaturation with SDS in Figure 2.

(B) Scheme for synthesis of **1*** by *N*-acylation of the starting oxazolidinone **4** with the mixed anhydride **3** to form **5**, reduction of the acetylene group of **5** with tritium gas to generate **6***, and isomerization of the resulting crotonyl group to yield **1***.

tectable binding activity in either nuclear or membrane fractions, as detected by fluorograms of sodium dodecyl sulfate (SDS)-polyacrylamide gels of [^{3}H]locostatin-treated samples (Figure 2 and data not shown). Modification of each protein by [^{3}H]locostatin could be competed away by coincubation with 50-fold molar excess of unlabeled locostatin over [^{3}H]locostatin, and we detected no other saturable and specific [^{3}H]locostatin binding proteins in MDCK cell extracts. The compound also labels these proteins when live cells are treated before lysis, showing that locostatin is cell permeant and can react with the same targets in vivo (data not shown). The compound's effects on cells are reversible, however, most likely as a result of new target biosynthesis following wash out [1]. The approximate molecular weights of these locostatin binding proteins are 21, 30, 55, and 80 kDa. On the basis of the association of each protein with [^{3}H]locostatin, we purified all four of these locostatin binding proteins from MDCK cell lysates. We determined the identity of these proteins by microcapillary HPLC-linear ion trap tandem mass spectrometry (MS) as: (1) the signaling modulator RKIP (~21 kDa); (2) the mechanistically novel glutathione *S*-transferase (GST) omega 1-1, or GSTO1-1 (~30 kDa); (3) aldehyde dehydrogenase 1A1, or ALDH1A1 (~55 kDa); and (4) prolyl oligopeptidase (POP), also known as prolyl endopeptidase (~80 kDa). In addition to isolation and identification of the proteins from MDCK cell lysates, we purified ALDH1A1 from A549 cells and bovine liver. We also expressed the cloned recombinant genes for RKIP, GSTO1-1, and POP.

Locostatin Reveals the Role of RKIP in Cell Migration

The reaction of [^{3}H]locostatin with RKIP is saturable and specific, since it is competed away with a 50-fold molar excess of unlabeled compound added simultaneously with [^{3}H]locostatin in both samples for MDCK cell extracts (Figure 2A) and bacterially expressed recombinant rat RKIP (Figure 2B). We calculated the second-order rate constant for association of locostatin with RKIP as 13.09 M^{-1} s^{-1} (Table S2). Furthermore, binding competition experiments performed with a series of unlabeled locostatin analogs show a correlation between the antimigratory activity of the analogs and their ability to compete with [^{3}H]locostatin for binding to RKIP (Figure 2B and Table 1), implying that RKIP may be a physiologically relevant target of locostatin. In addition, the fact that some of the cytotoxic compounds lacking any subtoxic effect do not compete well with [^{3}H]locostatin for binding to RKIP shows that

Table 1. Structure-Activity Relationships

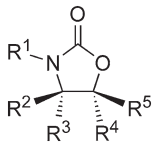

Compound	R^1	R^2	R^3	R^4	R^5	IC_{50}/Activity
1 (locostatin)		H	Bn	H	H	17.9 μM[a] (96%, 50 μM)[b]
7		H	Bn	H	H	no activity
8	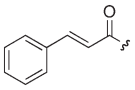	H	Bn	H	H	slight activity at 20 μM only (49%)[b]; toxic at ≥50 μM
9		H	i-Pr	H	H	39.5 μM[a] (78%, 100 μM)[b]
10	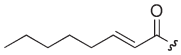	H	Bn	H	H	toxic at ≥100 μM[c]
11		H	Me	H	Ph	22.6 μM[a] (60%, 50 μM)[b]
12		H	Ph	H	H	23.7 μM[a] (83%, 50 μM)[b]
13	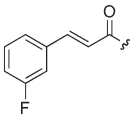	H	Bn	H	H	slight activity at 5 μM only (36%)[b]; toxic at ≥10 μM
14		Bn	H	H	H	toxic at ≥100 μM[c]
15		H	Bn	H	H	toxic at ≥50 μM[c]
16	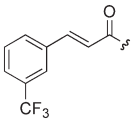	H	Bn	H	H	slight activity at 500 nM only (24%)[b]; toxic at ≥1 μM
17		H	Bn	H	H	81.5 μM[a] (31%, 1 mM)[b]
18	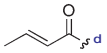 [d]	H	Bn	H	H	slight activity at 100 μM only (42%)[b]; toxic at ≥200 μM
thiazolidinethione analog						

[a] All IC_{50} values were calculated for inhibition of wound closure at the indicated times postwounding with normalization to parallel controls by using ≥5 different subtoxic concentrations in concentration-response experiments. Each concentration for each cell type and assay involved at least three separate experiments and was considered a bioactive concentration if there was statistically significant inhibition with $p < 0.05$ by an unpaired two-tailed Student's t test. All experiments were performed in serum-containing medium, unless otherwise noted. Our previously published value for the IC_{50} of locostatin based on percent inhibition of wound closure at 12 hr postwounding was 14 μM [1].
[b] Values in parentheses represent the percent inhibition of wound closure at 24 hr postwounding normalized to parallel controls for the highest subtoxic concentrations, as indicated. The higher the percentage, the more inhibitory the compound is at 24 hr relative to the parallel controls.
[c] Compounds labeled simply as toxic were cytotoxic starting at the indicated concentration but had no subtoxic inhibitory activity at any lower concentration in wound closure assays. Toxicity was defined on the basis of rounding up of cells and Trypan blue staining. The values in parentheses represent the minimum lethal concentration for these compounds.
[d] **18**, the thiazolidinethione analog of locostatin, has a less electrophilic α,β-unsaturated *N*-crotonyl group than locostatin and so should be less reactive with any nucleophile.

modification of RKIP and cytotoxicity are not strictly linked.

Locostatin hinders the ability of RKIP to inhibit Raf-1 kinase in vitro, thereby restoring the kinase activity of Raf-1 (Figure 3A) and making it, to our knowledge, the first inhibitor of RKIP discovered. Locostatin has no direct effect on the activity of Raf-1 kinase alone in control experiments; however, it is weakly inhibitory of substrate phosphorylation at elevated concentrations of ≥1 mM, most likely as a result of nonspecific alkylation

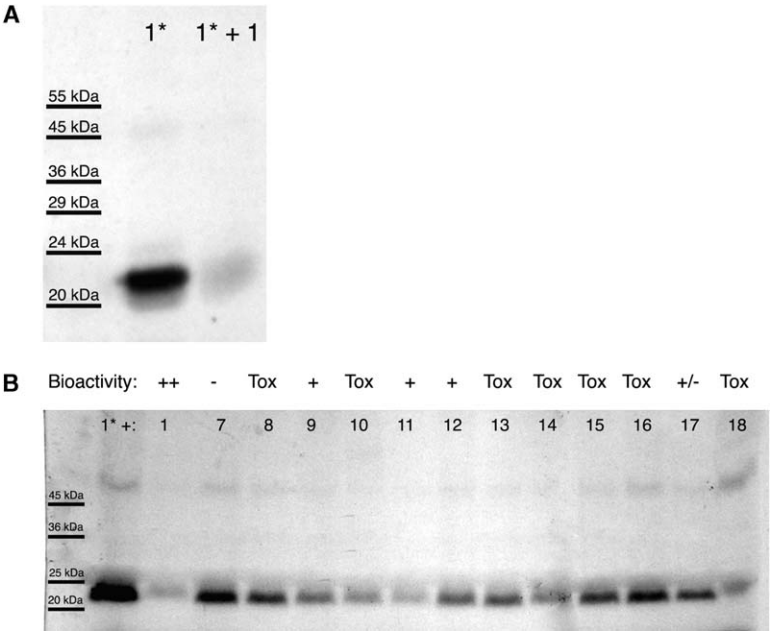

Figure 2. RKIP Is a Specific Target of Locostatin

(A and B) Fluorograms of SDS-polyacrylamide gels of (A) partially purified MDCK cell extracts or (B) recombinant rat RKIP treated with 1 μM [^{3}H]locostatin (**1***) for 3 hr, with or without 50 μM unlabeled locostatin (**1**) or unlabeled analogs **7–18** (structures in Table 1). The ~21 kDa locostatin binding protein was identified as RKIP by tandem MS following 2D gel electrophoresis of the partially purified samples from MDCK cell lysates. In (B), relative bioactivity in the MDCK wound closure assay for each locostatin analog is shown above the fluorogram. The compounds labeled "Tox" are cytotoxic starting at different concentrations (indicated in Table 1), but display little or no subtoxic effect on cell migration and wound closure. Identical results for [^{3}H]locostatin binding were obtained when treating live cells with [^{3}H]locostatin before cell lysis, demonstrating that the compound is membrane permeant and capable of modifying RKIP in vivo also.

at high concentrations. The mode of action of locostatin in the inactivation of RKIP involves disruption of the interaction between RKIP and Raf-1, with modification of RKIP by locostatin abolishing the ability of RKIP to bind Raf-1 (Figure 3B).

To further validate RKIP as a relevant target, we used RNAi to silence RKIP expression in MDCK cells (Figure 4A). Cells expressing a small interfering RNA (siRNA) targeting RKIP migrate more slowly than control cells (Figure 4B). The effect of RKIP knockdown recapitulates that of locostatin on cell migration. These results therefore further validate RKIP as the relevant target of locostatin, and they further implicate RKIP in cell migration.

We also performed the opposite manipulation, increasing rather than decreasing the levels of RKIP in MDCK cells, and evaluated the effect of overexpression of RKIP on the cells and their sensitivity to locostatin. We found dramatic changes in the morphology and migration of MDCK cells with RKIP overexpression (Figure 5). The RKIP-overexpressing cells grow without much cell-cell contact, like fibroblasts, rather than as islands in which cells strongly adhere to each other, like normal MDCK cells. Upon scratch wounding of confluent monolayers, normal MDCK cells migrate collectively as a continuous sheet, never losing their cell-cell contacts in the manner characteristic of strongly cell-cell adherent differentiated epithelial cells (Figure 5A and [16, 17]). In contrast, after wounding of confluent monolayers of MDCK cells that are overexpressing RKIP, migrating cells break away from the sheet, crawling as individual single cells not adhering to one another (Figure 5B), rather than collectively. This change is reminiscent of what occurs upon treatment of subconfluent MDCK cell cultures with HGF/SF, which results in conversion of the cells to a migratory and dispersing fibroblast-like phenotype (for a review, see [18]). It is accompanied by loss of cell-cell adhesions such as adherens junctions, which depend on E-cadherin, the primary cell adhesion molecule in MDCK [19, 20] and other epithelial cells (for reviews, see [21, 22]). The change in phenotype resembles the epithelial-mesenchymal transition (EMT) that certain epithelial cells undergo during embryonic development and in the progression of many epithelial cancers, and HGF/SF-treated MDCK cells have been widely used as a model for EMT (for reviews, see [23, 24]).

Treatment with locostatin appears to cause a morphological change of the RKIP-overexpressing MDCK cells to a less elongated and more cell-cell adhesive state (Figure 5D); however, this is not a complete reversion of cells back to a normal cuboidal epithelial phenotype, perhaps because of the relatively short time of exposure to locostatin, the high level of RKIP expression under the control of the human cytomegalovirus (CMV) promoter, or the simultaneous inhibition of the compound's other targets. It would have been interesting to grow the RKIP-overexpressing cells in the presence of locostatin; however, this was not possible since locostatin also inhibits cell proliferation [1]. However, the ability of locostatin to inhibit cell migration and wound closure is dramatically reduced when RKIP is overexpressed (Figure 6). There is little effect on the migration of RKIP-overexpressing cells with treatment of locostatin at subtoxic concentrations that strongly inhibit wound closure in control MDCK cells. At higher concentrations, locostatin is similarly toxic in both the RKIP-overexpressing MDCK cells and control cells. This suggests that the toxicity of the compound at higher concentrations is mediated by the inhibition of other targets, while the subtoxic antimigratory effect is due to the inhibition of RKIP. In addition, the RKIP-overexpressing cells tend to round up and die with long-term maintenance of the cultures at confluence, consistent with previous work showing that RKIP has proapoptotic activity in human prostate and breast cancer cells [25]. We found

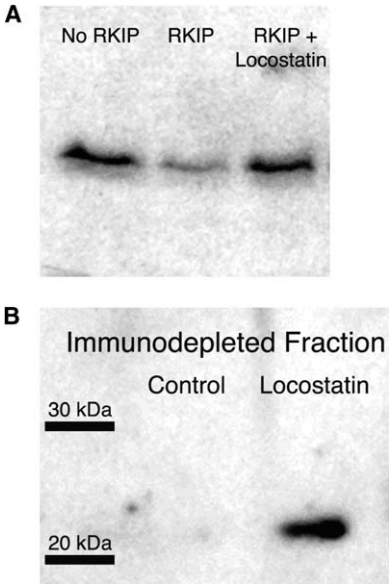

Figure 3. Locostatin Abrogates the Ability of RKIP to Inhibit the Kinase Activity of Raf-1 In Vitro by Preventing Interaction between the Two Proteins

(A) Locostatin hinders RKIP's ability to inhibit Raf-1 in vitro (100 μM locostatin; 3 hr of preincubation; control contains an equivalent volume percent of DMSO carrier solvent alone). Known amounts of expressed and purified recombinant RKIP (3.8 μg, which corresponds to 9 μM in the initial sample volume), activated Raf-1 (1 μl dilute purified sample), MEK1 (0.4 μg), and kinase-negative ERK2 (1.0 μg) were used in an in vitro Raf/MEK/ERK reaction sequence, as previously described [42], and equivalent amounts of sample were loaded onto the gel for each lane. The dominant band corresponds to the fraction of the fixed amount of kinase-negative ERK2 in each lane that has been ^{32}P-phosphorylated in the presence or absence of RKIP and locostatin. See Experimental Procedures for details. (Locostatin has no direct effect on the kinase activity of Raf-1 alone, although it weakly inhibits phosphorylation of MEK at ≥1 mM.)

(B) Alkylation of RKIP by locostatin prevents RKIP from interacting with Raf-1. RKIP preincubated with locostatin is not coimmunodepleted from solution with an anti-Raf-1 antibody in vitro (100 μM locostatin; 70 nM RKIP; 3 hr of preincubation; 20 μl volume in each case), as detected by Western blot analysis with an anti-RKIP antibody, while RKIP preincubated with DMSO alone is pulled out along with Raf-1 by the anti-Raf-1 antibody. The immunodepleted fraction is shown in both cases; therefore, the presence of an RKIP band means that the interaction with Raf-1 was inhibited by locostatin treatment.

The data in both (A) and (B) are representative of three separate experiments.

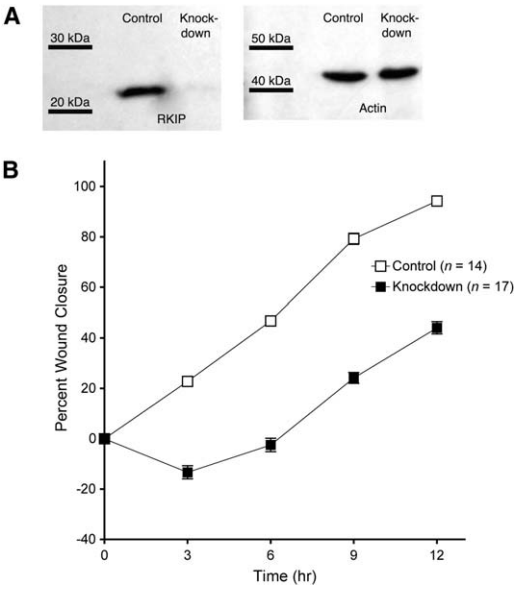

Figure 4. siRNA-Mediated Silencing of RKIP Expression Reduces the Rate of Migration of Epithelial Cells

(A) Western blot demonstrating knockdown of RKIP in MDCK cells expressing an siRNA corresponding to nucleotides 285–303 of the canine RKIP gene. The siRNA is expressed from a stably transfected expression vector described in Experimental Procedures. The control cells carry the same vector expressing an inert siRNA. Identical numbers of cells and amounts of total protein were loaded in both cases, as determined by counting cells with a hemocytometer before cell lysis and then Bradford assays after cell lysis. The loading control with anti-β-actin antibody is next to an anti-RKIP antibody probe; results are representative of three independent experiments.

(B) RKIP knockdown cells migrate more slowly than control cells in the wound closure assay (mean ± standard error of the mean for n wounds as indicated).

that treatment of the RKIP-overexpressing cells with locostatin protects them from death. Collectively, these data show that RKIP is the biologically relevant target of locostatin in MDCK cells and that RKIP is a critical regulator of epithelial cell migration.

Other Targets Not Involved in Cell Motility

We also investigated the effects of locostatin on the function of the other locostatin binding proteins and looked at the possible role of these proteins in wound closure. Locostatin inhibits ALDH1A1 with a second-order inactivation rate constant of 107.4 $M^{-1}s^{-1}$ (Table S2). However, when we tested four different available ALDH inhibitors (disulfiram, citral, *p*-chloromercuribenzoic acid, and cyanamide) for any effects on MDCK wound closure, we found no subtoxic inhibitory activity. These inhibitors compete with [^{3}H]locostatin for binding ALDH1A1 both in vitro and in vivo (the latter by short-term exposure of cells to [^{3}H]locostatin with or without high excess concentrations of unlabeled inhibitors, demonstrating that the inhibitors readily enter cells and bind cellular ALDH1A1). Therefore, inhibition of ALDH1A1 does not explain the effects of locostatin on MDCK cell migration, although it could still account for the toxicity of locostatin at higher concentrations. In addition, A549 cells, which contain much higher levels of ALDH1A1, are little affected in wound closure assays by locostatin at subtoxic concentrations.

Locostatin also inhibits POP with a second-order inactivation rate constant of 2.08 $M^{-1}s^{-1}$ (Table S2). However, treatment of MDCK cells with two available selective cell-permeant POP inhibitors, Z-Pro-Pro-CHO and Boc-Glu(NHO-Bz)-Pyr, which are extremely potent (pM and nM K_i values, respectively, for inhibition of POP), results in partial inhibition of wound closure only observed at very high concentrations (>200 μM), concentrations that are not far from where they become mani-

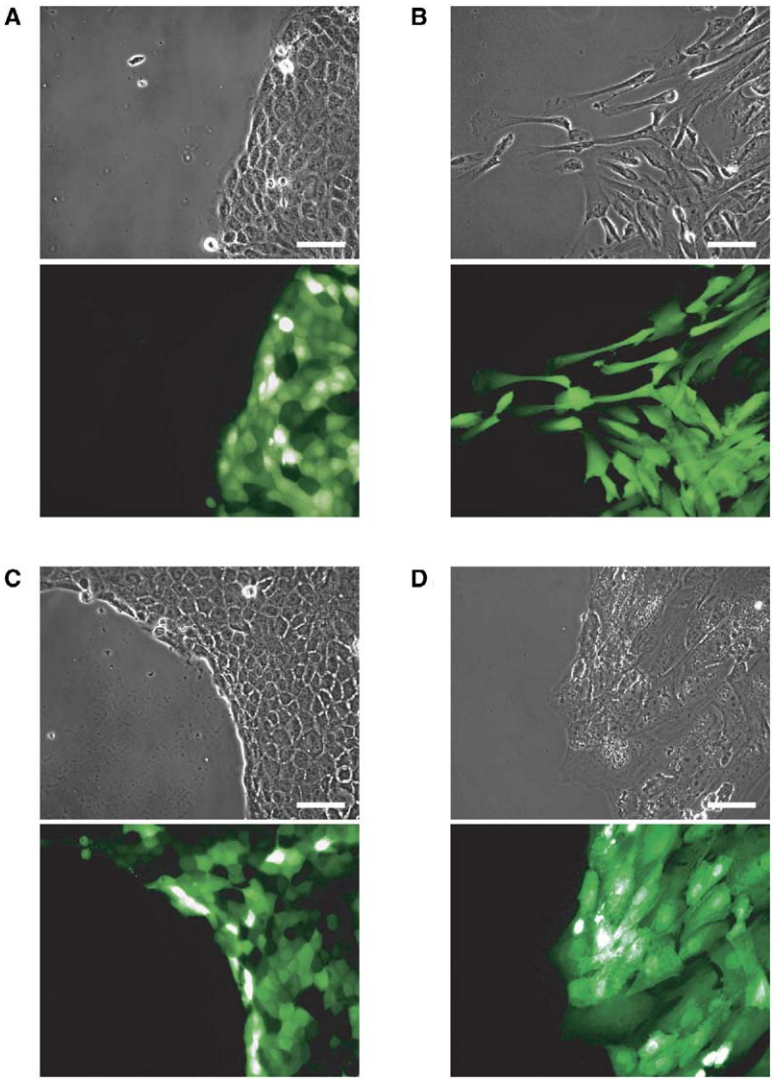

Figure 5. Overexpression of RKIP in Epithelial Cells Results in Conversion of Cells to a Fibroblast-Like Morphology

(A) Control MDCK cells stably transfected with EGFP alone.
(B) Stably transfected MDCK cells overexpressing RKIP-EGFP.
(C) Control stably EGFP-transfected MDCK cells treated with locostatin.
(D) Stably RKIP-EGFP-transfected MDCK cells treated with locostatin.
Treatments of confluent cell monolayers began 30 min before wounding (0.1% DMSO carrier solvent or 50 μM locostatin), and each monolayer was similarly scratch wounded and then imaged 6 hr after wounding. The fluorescence images show the high level of expression of (A and C) EGFP or (B and D) RKIP-EGFP, driven from the CMV promoter in the EGFP-C1 mammalian expression vector in both cases. Images are representative of at least three separate experiments in each case. Similar results were obtained following overexpression of hemagglutinin-tagged RKIP. Bars, 50 μm.

festly cytotoxic and thousands of times higher than their K_i values for inhibition of POP.

GSTO1-1 activity is also inhibited by locostatin, though extremely slowly, with second-order inactivation rate constants of 0.108 $M^{-1}s^{-1}$ in the DHA reductase assay and 0.063 $M^{-1}s^{-1}$ in the thiol transferase assay (Table S2), two assays of GSTO1-1 activity. However, again, treatment of MDCK cells with other GST inhibitors does not affect wound closure.

RKIP and POP are both unique proteins, although they are part of larger protein families: the PEBP and POP families, respectively. There are a number of ALDH and GST isoforms with different functions. We have not detected any other isoforms of either ALDH or GST as locostatin binding proteins by tandem MS, demonstrating the high degree of selectivity of locostatin for a single isoform of both enzyme classes. Both ALDH1A1 and GSTO1-1 have probable in vivo xenobiotic-metabolizing activities, like many of the better-characterized isoforms of these proteins.

RKIP and Cell Migration

Our results strongly suggest that RKIP is the only protein among the four locostatin binding proteins that plays a role in epithelial cell sheet migration during wound closure. Locostatin is the only inhibitor of RKIP discovered to date and acts by disrupting RKIP's ability to bind and inhibit Raf-1 kinase. It is unclear at this time how this inhibition leads to arrest of cell motility. Inhibition of RKIP could result in inappropriate stimulation of Raf-1, leading to activation of the MEK/ERK pathway, which may negatively regulate migration of MDCK cell sheets. We have previously found that the MEK inhibitors PD98059 and U0126 have little or no effect on wound closure in MDCK cell monolayers [26], but we have not analyzed the opposite manipulation, where the pathway is overactivated. It seems more likely, however, that the major part of RKIP's role in the regulation of cell migration results from inhibition of other effectors that could be downstream of Raf-1, apart from the MEK/ERK pathway, or else modulation of the activity of proteins other than Raf-1, such as GRK2 or another RKIP-regulated protein. Locostatin may also interfere with RKIP's ability to bind some other ligand, such as phosphatidylethanolamine, which could be important for epithelial cell migration.

RKIP is not itself an enzyme, but a nonenzymatic reg-

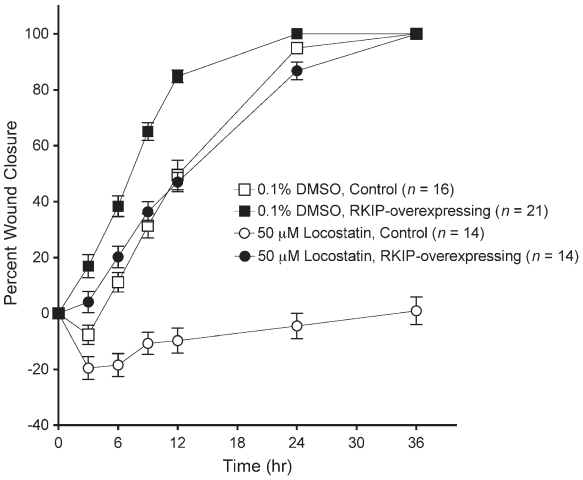

Figure 6. Overexpression of RKIP Dramatically Reduces the Antimigratory Effect of Locostatin and Results in More Rapid Cell Migration

Cells overexpressing RKIP are no longer significantly inhibited in wound closure assays by concentrations of locostatin at or below 50 μM, and they migrate faster than control cells (mean ± standard error of the mean for n wounds as indicated). In contrast, locostatin inhibits wound closure in normal MDCK cells down to 2 μM. Above 50 μM, locostatin becomes cytotoxic in the RKIP-overexpressing MDCK cells, as in control cells, suggesting that the toxicity at higher concentrations is mediated by the inhibition of other targets, while the antimigratory effect at subtoxic concentrations is mediated by the inhibition of RKIP. In addition, locostatin protects the RKIP-overexpressing cells from death with long-term culture, which we have found occurs without locostatin treatment (data not shown).

ulator of multiple kinases that acts through protein-protein interactions. Alkylation of RKIP by locostatin prevents it from binding Raf kinase either by directly targeting the protein-protein interaction interface or by an allosteric mechanism that alters the conformation of the interface region of RKIP. Although there is great interest in the development of compounds like locostatin that disrupt protein-protein interactions, particularly between signaling proteins, this is still a relatively uncommon mode of action for small-molecule inhibitors, the majority of which target enzyme active sites (for reviews, see [27–37]). Ser153 of RKIP can be phosphorylated by PKC, resulting in dissociation from Raf-1 and association with and inhibition of GRK2 [9]. In experiments testing whether this nucleophilic residue could be modified by locostatin, we found that preincubation of RKIP with locostatin does not affect the level of phosphorylation of RKIP by PKC (data not shown). Moreover, mutation of Ser153 to Ala does not affect the level of alkylation at saturation of RKIP by [^{3}H]locostatin (data not shown). These results suggest that locostatin does not modify Ser153. We are now investigating the detailed molecular mechanism of action of locostatin and the role of RKIP in regulating migration of the epithelial cell sheet during wound closure.

Recently, RKIP expression was found to be higher in a tumorigenic and metastatic murine fibrosarcoma cell line than in the weakly tumorigenic and nonmetastatic parental cell line from which it derives [38]. However, in contrast, RKIP levels are low in human prostate and breast cancer cells [15, 25], as well as in human melanoma cells, where overexpression of RKIP partially inhibits B-Raf-mediated, anchorage-independent growth [10]. Moreover, overexpression of RKIP reduces the invasiveness of human prostate cancer cells in vitro and appears to suppress metastasis in vivo by decreasing angiogenesis and vascular invasion [15]. Such activity appears to be opposite to that in MDCK epithelial cells, in which RKIP overexpression converts the cells to a fibroblast-like morphology and promotes migration. These different results cannot as yet be reconciled. They may indicate diverse and context-dependent functions for RKIP in the positive and negative control of cell motility, leading to the possibility that RKIP could function in different ways to either promote or suppress invasion and metastasis, depending on the type of cancer.

Significance

Using a small-molecule inhibitor, we have discovered that RKIP is necessary for the collective migration of epithelial cells. This compound inhibits epithelial cell migration and prevents RKIP from associating with and inhibiting Raf-1 kinase by disrupting the protein-protein interaction between RKIP and Raf-1. Silencing of RKIP expression by using RNAi also decreases the rate of cell migration. Overexpression of RKIP causes transformation of epithelial cells to a fibroblast-like phenotype, resulting in dispersion and migration of the cells as individuals. Furthermore, these results raise the possibility that initiation of collective migration of an epithelial cell sheet could itself represent a partial temporary transition to a more mesenchymal state, with acquisition of a more "invasive" character, but without loss of cell-cell contacts. To our knowledge, RKIP has not been shown to play a positive role in cell migration before this study, and, therefore, these results open up a new avenue for research on RKIP and cell motility.

Experimental Procedures

Synthesis of [^{3}H]Locostatin and Locostatin Analogs

[^{3}H]Locostatin (**1***, 58 Ci mmol^{-1}) was synthesized from the corresponding acetylene **5**, which was itself prepared by a previously described procedure [1], as were the other analogs used in this study. The structure and purity of all compounds were confirmed by nuclear magnetic resonance (NMR) and high-resolution mass spectrometry (HRMS).

Briefly, for synthesis of **5**, 2-butynoic acid (**2**, 70.62 mg, 0.84 mmol), trimethylacetyl chloride (101.2 mg, 0.84 mmol), and triethylamine (96.4 mg, 0.96 mmol) were dissolved in tetrahydrofuran (THF), cooled to −78°C, and stirred for 1 hr. The temperature was raised to 0°C, and the solution was stirred for 1 hr. The liquid mixture containing the mixed anhydride **3** was added dropwise to a solution of (4*S*)-(-)-benzyl-2-oxazolidinone (**4**, 100 mg, 0.56 mmol) and n-butyllithium (1.6 M in hexanes, 0.36 ml, 0.56 mmol) in THF that had been cooled to −78°C and stirred for 30 min. The reaction mixture was stirred at −78°C for 1 hr and allowed to warm to room temperature. The reaction was quenched with a saturated NH_4Cl solution and diluted with ethyl acetate and washed twice with H_2O and once with brine. The organic layer was dried over Na_2SO_4 and evaporated under reduced pressure. The product was purified by flash chromatography with silica gel using ethyl acetate:hexanes (1:1) as eluent. **5** (102.6 mg, white solid) was obtained, as verified by NMR. **6*** was prepared from **5** by reduction of the acetylene with tritium gas as follows. **5** (12 mg, 0.05 mmol) was dissolved in ethyl acetate, and Lindlar catalyst (2 mg) was added. The system was

flushed with carrier-free $^3H_2$ and sealed (6.5 inch mercury vacuum). The reaction mixture was stirred at room temperature for 5 hr. **6*** was purified with preparative thin layer chromatography (TLC) with a specific activity of 58 Ci mmol^{-1}. **1*** was then prepared from **6*** by isomerization of the crotonyl group. For this, **6*** was dissolved in CCl_4, and a small crystal of diphenyl disulfide was added. The reaction vessel was flushed with argon gas and fitted with a condenser, and an argon gas balloon was attached. The reaction mixture was irradiated with a projector lamp (70 volts, 60 watts) for 1.5 hr. The resulting **1*** was purified by preparative TLC, and its structure was established by NMR.

Locostatin (**1**, prepared by reduction of **5** to **6** with H_2 and isomerization to **1**, as described above for **1***): white solid; m.p. 83–84°C; ^{1}H NMR (500 MHz, $CDCl_3$): δ 7.34–7.21 (m, 7H, Ph, CH=CH), 4.75–4.70 (m, 1H, CHN), 4.22–4.16 (m, 2H, CH_2O), 3.33 (dd, 1H, J = 3.4, 13.4 Hz, C*H*HPh), 2.80 (dd, 1H, J = 9.6, 13.4 Hz, CH*H*Ph), 1.99 (dd, 3H, J = 0.9, 6.3 Hz, CH_3) ppm; ^{13}C NMR (100 MHz, $CDCl_3$): δ 164.87, 153.36, 146.93, 135.28, 129.37, 128.85, 127.22, 121.75, 66.01, 55.20, 37.79, 18.50 ppm; HRMS (EI) m/z calcd for $C_{14}H_{15}NO_3$ $[M]^+$ 245.1052, found 245.1060.

Cell Culture and Cell Migration Assays

MDCK cells were grown to confluence in minimum essential medium (MEM) supplemented with 10% newborn calf serum (NCS) and then scratch wounded and analyzed as previously described [1]. Because the RKIP-overexpressing MDCK cells migrated as individuals following wounding of confluent monolayers, the open area was determined by tracing the edge of the remaining intact cell monolayer, as for wounds in normal MDCK cell sheets, but then subtracting the area occupied by cells migrating into the wound area as individuals to obtain the correct unoccupied area as a function of time. Curve fitting and statistical analyses were done by using GraphPad Prism software.

Isolation of Protein Targets

Confluent MDCK cell monolayers were rinsed with phosphate-buffered saline (PBS) thrice and incubated on ice for 30 min in lysis buffer consisting of 20 mM Tris-HCl (pH 7.4), 150 mM NaCl, 0.1% Sigma protease inhibitors cocktail solution for mammalian cell and tissue extracts, 0.5% Triton X-100, and 2 mM dithiothreitol (DTT). The cells were scraped off the plates and dounce homogenized. The crude extract was centrifuged at 15,000 × g for 30 min at 4°C, and then the supernatant was carefully decanted and saved for binding assays or further purification. Locostatin binding experiments were performed by adding [^{3}H]locostatin to small aliquots of the extract samples, followed by incubation at 16°C for 3 hr. Saturability and specificity of the reaction between locostatin and its binding proteins were determined by adding 50-fold molar excess of unlabeled locostatin simultaneously with [^{3}H]locostatin in binding competition experiments. After incubation, the sample was subjected to SDS-polyacrylamide gel electrophoresis (SDS-PAGE). The gel was stained with Coomassie blue, shaken in Amplify fluorography solution (Amersham) for 30 min, placed on filter paper, and dried. The dried gel was then exposed to Amersham Hyperfilm autoradiography film at –80°C, and the film was developed to visualize the proteins radioactively labeled by reaction with [^{3}H]locostatin.

[^{3}H]Locostatin binding assay-guided purification of the specific locostatin binding proteins was accomplished as follows. MDCK cell extracts in lysis buffer were dialyzed against 20 mM *bis*-Tris (pH 6.0), 2 mM DTT overnight and centrifuged at 15,000 × g for 30 min. The supernatant was applied to a HiTrap Q-sepharose column (Amersham Biosciences), and the flow-through was collected. Proteins were eluted from the column with a linear gradient of NaCl and set aside. The flow-through was then fractionated by progressive precipitation as 25%, 40%, 50%, 60%, and 80% ammonium sulfate pellets. Ammonium sulfate precipitates containing ~21, ~30, and ~55 kDa locostatin binding proteins were resuspended in PBS, desalted by centrifugation at 5,000 × g in Amicon (Millipore) centrifugal filter units with the addition of ultrapure H_2O, subjected to two-dimensional (2D) gel electrophoresis on a flatbed isoelectric focusing system (Scie-Plas), and stained with Coomassie brilliant blue R-250. In contrast to the other three proteins, the ~80 kDa locostatin binding protein bound to the Q-sepharose column; following elution, the ~80 kDa locostatin binding fractions were pooled, subjected to SDS-PAGE, and stained with Coomassie brilliant blue R-250. Each relevant protein band or spot was cleanly resolved on the gels and lined up with [^{3}H]locostatin binding proteins on fluorograms of parallel gels prepared as described above. All bands or spots corresponding to [^{3}H]locostatin binding activities were cut out from the gels.

Target Identification

Excised protein bands were subjected to in gel reduction, carboxyamidomethylation, and digestion with trypsin. Peptide sequences were determined by using a 75 μm reverse phase microcolumn terminating in a custom nanoelectrospray source (New Objective) directly coupled to an LTQ linear quadrupole ion trap mass spectrometer (Thermo Electron). The instrument was operated in data-dependent mode, fragmenting (relative collision energy = 30%, isolation width = 2.5 Da, dynamic exclusion on) the four most abundant ions in each survey scan. Preliminary sequencing of peptides was facilitated by correlation of the National Center for Biotechnology Information (NCBI) nr database with the algorithm SEQUEST [39], an in-house spectrum review workbench, FuzzyIons, and neural network ScoreFinal. All protein assignments met the following criteria: (i) a minimum of four unique peptide sequences; (ii) a minimum of ten MS/MS-acquired spectra allowing for redundant sequences; (iii) a ScoreFinal $\geq$ 0.83. ScoreFinal is a single Sequest score that we developed; is implemented in Sequest Browser v. 3.2; and is the output, normalized to 1.00, of a neural network (with one hidden layer) whose inputs are the five Sequest scores (XCorr, dCn, Sp, rSp, and Ions), peptide charge state, mass, and database size. Evaluation with a reverse NCBI nr database reveals a peptide false positive rate of < 0.5% when ScoreFinal > 0.8. Finally, (iv) all spectra were manually inspected for completeness of ion assignments and intensity-based signatures, e.g., neutral loss(es), proline ions, etc.

Expression and Purification of Recombinant Genes

We expressed recombinant genes in *Escherichia coli* (DH5α or JM109 strains) following $CaCl_2$-mediated transformation of the bacteria. Rat RKIP fused to GST in the pGEX-KG vector was expressed and purified as previously described [6]. His_6-tagged GSTO1-1 in pQE30 was expressed and purified as previously described [40]. His_6-tagged POP in pCHH29 was also expressed and purified as previously described [41]. The Raf-1 kinase assay involved multiple recombinant kinases: Raf-1, a kinase-negative mutant of extracellular signal-regulated kinase 2 (ERK2) and mitogen-activated protein kinase/ERK kinase 1 (MEK1). GST-Raf-1 in pEBG, GST-MEK1 in pGEX-KG, and GST-ERK2 in pGEX-KG were expressed and purified as previously described [42]. The GST-Raf-1-containing construct was transfected into COS-7 cells by using lipofectamine and was activated by treating the cells with 100 nM phorbol 12-myristate 13-acetate for 15 min before cell lysis. GST-Raf-1 was purified by using glutathione-agarose beads and was eluted from the beads with 10 mM reduced glutathione. GST was cleaved from all of the recombinant proteins with thrombin.

Purification of ALDH1A1

ALDH1A1 was purified from MDCK cells, A549 cells, and bovine liver on the basis of [^{3}H]locostatin binding assays performed with samples of each fraction. Purification from MDCK cells involved Q-sepharose column chromatography (pH 6.0, collection of [^{3}H]locostatin binding activity in the flow through), ammonium sulfate precipitation (50%–60% fraction), gel filtration (the ALDH1A1 tetramer is ~220 kDa), and phenyl hydrophobic column chromatography. For purification from A549 cells, the scheme involved Q-sepharose column chromatography (pH 8.0, elution at 200–400 mM NaCl), ammonium sulfate precipitation (50%–60% fraction), gel filtration, and phenyl hydrophobic column chromatography. For purification from bovine liver, the sequence entailed ammonium sulfate precipitation (50%–70% fraction), Q-sepharose column chromatography (pH 8.0, elution ~200 mM NaCl), hydrophobic column chromatography, and gel filtration. All steps were done at 4°C.

Raf Kinase Enzyme Assay

The assay involves in vitro reconstitution of the Raf/MEK/ERK cascade as previously described [42]. A total of 3.8 μg purified recombinant RKIP, corresponding to 9 μM in the initial sample volume, was preincubated at 16°C for 3 hr with 100 μM locostatin, or an equivalent volume percent of dimethyl sulfoxide (DMSO) carrier solvent alone, in 20 μl kinase buffer (40 mM Tris-HCl [pH 7.5], 0.1 mM EDTA, 5 mM $MgCl_2$, 2 mM DTT, 20 μM ATP). Activated Raf-1 (1 μl dilute purified sample) was then added to the solution. After incubation on ice for 30 min, 0.4 μg MEK1 and 10 μCi [^{32}P]γ-ATP were added, followed by incubation at 37°C for 30 min. MEK1 ^{32}P-phosphorylation is not readily detectable on autroradiograms, so in a subsequent kinase "signal amplification" step, 1.0 μg kinase-negative ERK2, a substrate of MEK1, was added to the reaction mixture with incubation for another 30 min at 37°C. The reaction was stopped by the addition of SDS sample buffer and was then subjected to SDS-PAGE. After staining with Coomassie blue, the gel was dried and exposed to autoradiography film for detection of ^{32}P-phosphorylated ERK2.

RKIP-Raf-1 Binding

70 nM RKIP was preincubated with 100 μM locostatin or DMSO carrier solvent alone at 16°C for 3 hr, then mixed with activated Raf-1 in kinase buffer and incubated on ice for 30 min. A total of 2 μg rabbit anti-Raf-1 antibody (Santa Cruz Biotechnology) was added for incubation at 4°C for 2 hr with rotation. A total of 10 μl of a 50% slurry of protein A-sepharose 4B beads (Zymed) was added for further incubation at 4°C for 1 hr with rotation. The beads were pelleted by centrifugation at 10,000 × g for 5 s. The supernatant was carefully removed and subjected to SDS-PAGE, followed by Western blot analysis with mouse anti-RKIP antibody (Zymed) and chemiluminescent detection with goat anti-mouse IgG conjugated to horseradish peroxidase (Santa Cruz Biotechnology).

ALDH1A1 Enzyme Assay

ALDH1A1 purified from cultured A549 cells, in which it is highly expressed, was added to a final concentration of ~67 nM to the assay mixture (100 mM Tris-HCl [pH 8.0], 100 mM KCl, 11 mM β-mercaptoethanol, 6.7 mM NAD^+, 3.3 mM acetaldehyde). Absorbance at 340 nm was measured at 1 min intervals for 30 min at 25°C. Reaction progress curves were linear in the initial phase in this and the subsequent enzyme assays, and these were used to calculate the rates of the enzyme reactions in all cases.

POP Enzyme Assay

The fluorogenic substrate Z-Gly-Pro-aminomethylcoumarin was used as POP substrate in the assay buffer (20 mM Tris-HCl [pH 7.3], 1 mM EDTA, 1 mM DTT). The release of fluorescent AMC upon addition of POP at 25°C was monitored by using excitation and emission wavelengths of 381 nm and 455 nm, respectively, at 30 s intervals for 10 min on an Flx800 microplate fluorescence reader from Bio-Tek Instruments.

GSTO1-1 Enzyme Assay

The DHA reductase and thiol transferase activities of GSTO1-1 were assayed. DHA reductase activity was assayed in 100 mM Tris-HCl (pH 8.0), 1 mM reduced glutathione, 0.25 mM DHA, to which GSTO1-1 was added to a final concentration of 1 μM. Starting 10 s after the addition of GSTO1-1, absorbance at 265 nm was measured at 5 s intervals for 10 min at 25°C. The thiol transferase activity was assayed in 100 mM Tris-HCl (pH 8.0), 0.5 mM reduced glutathione, 1 mM 2-hydroxyethyl disulfide, 0.4 mM NADPH, 1 U glutathione reductase. Beginning 10 s after the addition of GSTO1-1 to 1 μM, absorbance at 340 nm, which decreases with oxidation of NADPH, was measured at 30 s intervals for 10 min at 25°C.

Kinetics of Association of Locostatin with Proteins

The pseudo-first-order rate constant, k_{obs}, was determined by plotting the natural logarithm of the residual enzyme activity or the fractional saturation as a function of time, then calculating the slope of the line, which corresponds to $-k_{obs}$. The second-order rate constant (known as k_{assoc} or k_{inact}) for the inhibition of each protein by locostatin was calculated by using the relationship $k_{assoc} = k_{obs}/[I]$, where [I] is the locostatin concentration. In this way, the k_{assoc} was determined for the inactivation of ALDH1A1, GSTO1-1, and POP by locostatin. In all of these experiments, ≥100× excess of locostatin over the concentration of each enzyme was used to ensure pseudo-first-order conditions. The proteins were incubated with locostatin at 25°C for different lengths of times prior to dilution in the respective assay mixtures. Residual enzyme activities were then measured. To determine the kinetics of alkylation of RKIP by locostatin, 1 μM recombinant RKIP was incubated with 100 μM locostatin (a mixture of 20 μM [^{3}H]locostatin and 80 μM unlabeled locostatin) for different lengths of time at 25°C in 50 mM Na_2PO_4 (pH 8.0), 2 mM EDTA, 2 mM DTT, followed by SDS-PAGE. The gel was stained with Coomassie blue, and the region of the gel containing RKIP around 21 kDa was excised and dissolved for scintillation counting. By 2 hr of incubation with [^{3}H]locostatin at 25°C, saturation binding of RKIP had been attained. We plotted the natural logarithm of the fractional saturation of RKIP as a function of time (between 0 hr and 2 hr) to obtain k_{obs}, and then calculated k_{assoc} as described above.

Cloning, Silencing, and Overexpression of Canine RKIP in MDCK Cells

We cloned the canine RKIP gene, amplifying it from MDCK cell cDNAs by the polymerase chain reaction with Pfu DNA polymerase by using primers 5′-CCGCTCGAGCGGCTATGCCGGTGGACCTCG GCAAG-3′ and 5′-GCTCTAGAGCACTGCCCTACTTCCCAGACAGC-3′. Subsequent DNA sequencing confirmed identity with the predicted gene from dog genomic sequence (GenBank accession number XM 534698).

We constructed an RNA polymerase II-directed siRNA expression vector from the pTRE2hyg vector for use in the Tet-Off inducible system (BD Biosciences Clontech), guided by previous publications [43–45]. The EGFP expression cassette from the pEGFP-C1 mammalian expression vector was inserted between the ApaI and BglII restriction sites of pTRE2hyg at nucleotide positions 1086 and 1255, respectively. A new BamHI site was introduced immediately after position 371 of the modified pTRE2hyg. We synthesized an optimized SV40 poly-A signal sequence, based on the poly-A signal sequence of the Ambion p*Silencer* 4.1-CMV RNA polymerase II-directed siRNA expression vectors, that included an SpeI site at the upstream end and a NotI site at the downstream end. This poly-A signal sequence was then introduced immediately upstream of the NotI site in the multiple cloning site of the modified vector.

Five different siRNAs were constructed as short hairpin RNAs (shRNAs, also known as hairpin siRNAs) corresponding to different target sequences in the canine RKIP gene, and each was inserted between the new BamHI and SpeI sites, just upstream of the new poly-A signal sequence. Expressed shRNAs are processed in the cell to siRNAs that silence or knock down expression of their targets (for review, see [46]). The structures of our cloned constructs were confirmed by DNA sequencing. Each construct was then transfected into Tet-Off MDCK cells (BD Biosciences Clontech) by using lipofectamine, according to the manufacturer's protocol (Invitrogen). Stable transfectants were selected and maintained in 400 μg/ml hygromycin B and 1 μg/ml doxycycline in MEM with 10% NCS, and EGFP-expressing cells were collected. Induction of each shRNA/siRNA was accomplished by withdrawing doxycycline from the medium. Knockdown was confirmed by Western blot analysis by using the same anti-RKIP antibody as described above and then mouse anti-β-actin antibody (Santa Cruz Biotechnology) as loading control. An shRNA/siRNA corresponding to nucleotides 285–303 of the canine RKIP gene was particularly effective at silencing RKIP expression and was therefore used for wound closure experiments. The control was an inert shRNA/siRNA in the same vector that did not affect expression of RKIP. After 4 days in the absence of doxycycline, cell monolayers were scratch wounded and then analyzed, as described earlier. While we found RKIP knockdown even in the presence of doxycycline, indicating "leakiness" of the modified Tet-Off system, this was not a problem since the cells displayed no obvious changes in growth rate or morphology despite silencing of RKIP expression.

For overexpression of RKIP, the canine RKIP gene was fused to

enhanced green fluorescent protein (EGFP) by ligation into the XhoI and XbaI restriction sites of the pEGFP-C1 mammalian expression vector, which drives insert fusion gene expression from the CMV immediate early promoter. After propagation in *E. coli*, the EGFP-RKIP construct was purified and sequenced to confirm its proper identity. The construct was then transfected into MDCK cells by using lipofectamine, as described above. Stable transfectants were selected and maintained in 500 μg/ml G418 sulfate in MEM with 10% NCS. Stable transfectants with empty pEGFP-C1 vector were also prepared as control cells.

Supplemental Data

Supplemental Data including Supplemental Experimental Procedures and two tables are available at http://www.chembiol.com/cgi/content/full/12/9/981/DC1/.

Acknowledgments

We thank Kam Yeung (Medical College of Ohio) for GST-RKIP, Philip Board (Jane Curtin School of Medicine, Australian National University) for His_6-tagged GSTO1-1, Dario Neri (Swiss Federal Institute of Technology Zurich) for His_6-tagged POP, and Zhi-Jun Luo (Boston University School of Medicine) for GST-Raf-1, GST-MEK1, and GST-ERK2 constructs. This work was supported by grants from the National Institutes of Health (CA095177) and the American Cancer Society (RZG-02-250-01-DDC) to G.F.

Received: May 5, 2005
Revised: June 17, 2005
Accepted: July 11, 2005
Published: September 23, 2005

References

1. Mc Henry, K.T., Ankala, S.V., Ghosh, A.K., and Fenteany, G. (2002). A non-antibacterial oxazolidinone derivative that inhibits epithelial cell sheet migration. ChemBioChem *11*, 1105–1111.
2. Fenteany, G., and Zhu, S. (2003). Small-molecule inhibitors of actin dynamics and cell motility. Curr. Top. Med. Chem. *3*, 593–616.
3. Keller, E.T., Fu, Z., and Brennan, M. (2005). The biology of a prostate cancer metastasis suppressor protein: Raf kinase inhibitor protein. J. Cell. Biochem. *94*, 273–278.
4. Trakul, N., and Rosner, M.R. (2005). Modulation of the MAP kinase signaling cascade by Raf kinase inhibitory protein. Cell Res. *15*, 19–23.
5. Odabaei, G., Chatterjee, D., Jazirehi, A.R., Goodglick, L., Yeung, K., and Bonavida, B. (2004). Raf-1 kinase inhibitor protein: structure, function, regulation of cell signaling, and pivotal role in apoptosis. Adv. Cancer Res. *91*, 169–200.
6. Yeung, K., Seitz, T., Li, S., Janosch, P., McFerran, B., Kaiser, C., Fee, F., Katsanakis, K.D., Rose, D.W., Mischak, H., et al. (1999). Suppression of Raf-1 kinase activity and MAP kinase signalling by RKIP. Nature *401*, 173–177.
7. Yeung, K., Janosch, P., McFerran, B., Rose, D.W., Mischak, H., Sedivy, J.M., and Kolch, W. (2000). Mechanism of suppression of the Raf/MEK/extracellular signal-regulated kinase pathway by the Raf kinase inhibitor protein. Mol. Cell. Biol. *20*, 3079–3085.
8. Corbit, K.C., Trakul, N., Eves, E.M., Diaz, B., Marshall, M., and Rosner, M.R. (2003). Activation of Raf-1 signaling by protein kinase C through a mechanism involving Raf kinase inhibitory protein. J. Biol. Chem. *278*, 13061–13068.
9. Lorenz, K., Lohse, M.J., and Quitterer, U. (2003). Protein kinase C switches the Raf kinase inhibitor from Raf-1 to GRK-2. Nature *426*, 574–579.
10. Park, S., Yeung, M.L., Beach, S., Shields, J.M., and Yeung, K.C. (2005). RKIP downregulates B-Raf kinase activity in melanoma cancer cells. Oncogene *24*, 3535–3540.
11. Trakul, N., Menard, R.E., Schade, G.R., Qian, Z., and Rosner, M.R. (2005). Raf kinase inhibitory protein regulates Raf-1 but not B-Raf kinase activation. J. Biol. Chem. *280*, 24931–24940.
12. Yeung, K.C., Rose, D.W., Dhillon, A.S., Yaros, D., Gustafsson, M., Chatterjee, D., McFerran, B., Wyche, J., Kolch, W., and Sedivy, J.M. (2001). Raf kinase inhibitor protein interacts with NF-κB-inducing kinase and TAK1 and inhibits NF-κB activation. Mol. Cell. Biol. *21*, 7207–7217.
13. Bernier, I., Tresca, J.P., and Jolles, P. (1986). Ligand-binding studies with a 23 kDa protein purified from bovine brain cytosol. Biochim. Biophys. Acta *871*, 19–23.
14. Ojika, K., Mitake, S., Tohdoh, N., Appel, S.H., Otsuka, Y., Katada, E., and Matsukawa, N. (2000). Hippocampal cholinergic neurostimulating peptides (HCNP). Prog. Neurobiol. *60*, 37–83.
15. Fu, Z., Smith, P.C., Zhang, L., Rubin, M.A., Dunn, R.L., Yao, Z., and Keller, E.T. (2003). Effects of Raf kinase inhibitor protein expression on suppression of prostate cancer metastasis. J. Natl. Cancer Inst. *95*, 878–889.
16. Fenteany, G., Janmey, P.A., and Stossel, T.P. (2000). Signaling pathways and cell mechanics involved in wound closure by epithelial cell sheets. Curr. Biol. *10*, 831–838.
17. Farooqui, R., and Fenteany, G. (2005). Multiple rows of cells behind an epithelial wound edge extend cryptic lamellipodia to collectively drive cell-sheet movement. J. Cell Sci. *118*, 51–63.
18. Balkovetz, D.F. (1998). Hepatocyte growth factor and Madin-Darby canine kidney cells: in vitro models of epithelial cell movement and morphogenesis. Microsc. Res. Tech. *43*, 456–463.
19. Imhof, B.A., Vollmers, H.P., Goodman, S.L., and Birchmeier, W. (1983). Cell-cell interaction and polarity of epithelial cells: specific perturbation using a monoclonal antibody. Cell *35*, 667–675.
20. Behrens, J., Birchmeier, W., Goodman, S.L., and Imhof, B.A. (1985). Dissociation of Madin-Darby canine kidney epithelial cells by the monoclonal antibody anti-arc-1: mechanistic aspects and identification of the antigen as a component related to uvomorulin. J. Cell Biol. *101*, 1307–1315.
21. Braga, V.M. (2002). Cell-cell adhesion and signalling. Curr. Opin. Cell Biol. *14*, 546–556.
22. Perez-Moreno, M., Jamora, C., and Fuchs, E. (2003). Sticky business: orchestrating cellular signals at adherens junctions. Cell *112*, 535–548.
23. Thiery, J.P. (2003). Epithelial-mesenchymal transitions in development and pathologies. Curr. Opin. Cell Biol. *15*, 740–746.
24. Shook, D., and Keller, R. (2003). Mechanisms, mechanics and function of epithelial-mesenchymal transitions in early development. Mech. Dev. *120*, 1351–1383.
25. Chatterjee, D., Bai, Y., Wang, Z., Beach, S., Mott, S., Roy, R., Braastad, C., Sun, Y., Mukhopadhyay, A., Aggarwal, B.B., et al. (2004). RKIP sensitizes prostate and breast cancer cells to drug-induced apoptosis. J. Biol. Chem. *279*, 17515–17523.
26. Altan, Z.M., and Fenteany, G. (2004). c-Jun N-terminal kinase regulates lamellipodial protrusion and cell sheet migration during epithelial wound closure by a gene expression-independent mechanism. Biochem. Biophys. Res. Commun. *322*, 56–67.
27. McCormick, F. (2000). Small-molecule inhibitors of cell signaling. Curr. Opin. Biotechnol. *11*, 593–597.
28. Way, J.C. (2000). Covalent modification as a strategy to block protein-protein interactions with small-molecule drugs. Curr. Opin. Chem. Biol. *4*, 40–46.
29. Cochran, A.G. (2001). Protein-protein interfaces: mimics and inhibitors. Curr. Opin. Chem. Biol. *5*, 654–659.
30. Berg, T. (2003). Modulation of protein-protein interactions with small organic molecules. Angew. Chem. Int. Ed. Engl. *42*, 2462–2481.
31. Gadek, T.R., and Nicholas, J.B. (2003). Small molecule antagonists of proteins. Biochem. Pharmacol. *65*, 1–8.
32. Sandrock, T., and Kamb, A. (2003). Non-traditional drug targets: high risk, high reward. Curr. Gene Ther. *3*, 395–404.
33. Arkin, M.R., and Wells, J.A. (2004). Small-molecule inhibitors of protein-protein interactions: progressing towards the dream. Nat. Rev. Drug Discov. *3*, 301–317.
34. Pagliaro, L., Felding, J., Audouze, K., Nielsen, S.J., Terry, R.B., Krog-Jensen, C., and Butcher, S. (2004). Emerging classes of

protein-protein interaction inhibitors and new tools for their development. Curr. Opin. Chem. Biol. *8*, 442–449.
35. Arkin, M. (2005). Protein-protein interactions and cancer: small molecules going in for the kill. Curr. Opin. Chem. Biol. *9*, 317–324.
36. Yin, H., and Hamilton, A.D. (2005). Strategies for targeting protein-protein interactions with synthetic agents. Angew. Chem. Int. Ed. Engl. *44*, 4130–4163.
37. Zhao, L., and Chmielewski, J. (2005). Inhibiting protein-protein interactions using designed molecules. Curr. Opin. Struct. Biol. *15*, 31–34.
38. Hayashi, E., Kuramitsu, Y., Okada, F., Fujimoto, M., Zhang, X., Kobayashi, M., Iizuka, N., Ueyama, Y., and Nakamura, K. (2005). Proteomic profiling for cancer progression: differential display analysis for the expression of intracellular proteins between regressive and progressive cancer cell lines. Proteomics *5*, 1024–1032.
39. Eng, J.K., McCormack, A.L., and Yates, J.R., III. (1994). An approach to correlate tandem mass spectral data of peptides with amino acid sequences in a protein database. J. Am. Soc. Mass Spectrom. *5*, 967–989.
40. Whittington, A., Vichai, V., Webb, G., Baker, R., Pearson, W., and Board, P. (1999). Gene structure, expression and chromosomal localization of murine theta class glutathione transferase mGSTT1-1. Biochem. J. *337*, 141–151.
41. Heinis, C., Alessi, P., and Neri, D. (2004). Engineering a thermostable human prolyl endopeptidase for antibody-directed enzyme prodrug therapy. Biochemistry *43*, 6293–6303.
42. Tzivion, G., Luo, Z., and Avruch, J. (1998). A dimeric 14-3-3 protein is an essential cofactor for Raf kinase activity. Nature *394*, 88–92.
43. Gossen, M., and Bujard, H. (1992). Tight control of gene expression in mammalian cells by tetracycline-responsive promoters. Proc. Natl. Acad. Sci. USA *89*, 5547–5551.
44. Xia, H., Mao, Q., Paulson, H.L., and Davidson, B.L. (2002). siRNA-mediated gene silencing *in vitro* and *in vivo*. Nat. Biotechnol. *20*, 1006–1010.
45. Kojima, S., Vignjevic, D., and Borisy, G.G. (2004). Improved silencing vector co-expressing GFP and small hairpin RNA. Biotechniques *36*, 74–79.
46. Paddison, P.J., Caudy, A.A., Sachidanandam, R., and Hannon, G.J. (2004). Short hairpin activated gene silencing in mammalian cells. Methods Mol. Biol. *265*, 85–100.

Accession Numbers

The canine RKIP cDNA sequence has been deposited in the GenBank database under the accession number DQ130016.